ELSEVIER

Materials Science and Engineering B81 (2001) 3–8

MATERIALS SCIENCE & ENGINEERING B

www.elsevier.com/locate/mseb

Exciton–erbium energy transfer in Si nanocrystal-doped SiO_2

P.G. Kik, A. Polman *

FOM — Institute for Atomic and Molecular Physics, Kruislaan 407, 1098 SJ Amsterdam, The Netherlands

Abstract

Silicon nanocrystals were formed in SiO_2 using Si ion implantation followed by thermal annealing. The nanocrystal-doped SiO_2 layer was implanted with Er to peak concentrations ranging from 0.015 to 1.8 at.%. Upon 458 nm excitation, a broad nanocrystal-related luminescence spectrum centered around 750 nm and two sharp Er luminescence lines at 982 and 1536 nm are observed. By measuring the temperature-dependent intensities and luminescence dynamics at a fixed Er concentration, and by measuring the Er concentration dependence of the nanocrystal and Er photoluminescence intensity, the nanocrystal excitation rate, the Er excitation and decay rate, and the Er saturation with pump power we conclude that: (1) the Er is excited by excitons recombining within Si nanocrystals through a strong coupling mechanism; (2) the exciton–Er energy transfer rate is $>10^6$ s^{-1}; (3) the exciton–Er energy transfer efficiency is >60 %; (4) each nanocrystal can have at most ~ 1–2 excited Er ions in its vicinity, which is attributed to either an Auger de-excitation or a pair-induced quenching mechanism; (5) at a typical nanocrystal concentration of 10^{19} cm^{-3}, the maximum optical gain at 1.54 μm of an Er-doped waveguide amplifier based on Si nanocrystal-doped SiO_2 is ~ 0.6 dB cm^{-1}; (6) the effective Er excitation cross-section using this nanocrystal sensitization scheme is $\sigma_{eff} \approx 10^{-15}$ cm^2 at 458 nm, which is a factor 10^5–10^6 larger than the cross-section for direct optical pumping of Er. This enables the fabrication of an Er-doped nanocrystal waveguide amplifier that can be pumped using a white light source.

Keywords: Erbium; Nanocrystal; Exciton; Energy transfer; Optical waveguide; Optical amplifier

1. Introduction

Erbium-doped silica glass is used in optical telecommunications technology as an amplification medium. The Er^{3+} ions in the glass matrix exhibit a number of sharp emission lines due to electronic transitions within the 4f shell. The transition from the first excited state to the ground state occurs around 1540 nm, a standard wavelength in optical telecommunications. Optical amplification at this wavelength can be achieved if sufficient Er can be brought into the first excited state. Unfortunately, the optical cross-sections for the intra-4f transitions are rather small, typically on the order of 10^{-21} cm^2. For this reason there is considerable interest in sensitizing the Er^{3+} ions by adding a strongly absorbing species that can transfer energy efficiently to Er.

Recently, Fujii et al. reported that the presence of Si nanocrystals in Er-doped SiO_2 considerably enhances the effective Er absorption cross-section [1]. Following this observation, a number of articles appeared that showed similar results for similar materials prepared using different techniques [2–5]. All observations strongly suggest that energy is transferred from Si nanocrystals to the Er. A possible excitation model is shown in Fig. 1(a), which shows a schematic band diagram of SiO_2 containing a Si nanocrystal and Er^{3+}. First a photon is absorbed by the nanocrystal, which causes generation of an exciton bound in the nanocrystal. This exciton can recombine radiatively, emitting a photon with an energy that depends on the nanocrystal size. If an Er ion is present close to the nanocrystal, the exciton can recombine non-radiatively by bringing Er into one of its excited states.

Although the excitation model sketched in Fig. 1(a) is often referred to, the following issues have not been resolved: (1) the *lifetime paradox:* recently Franzò et al. [5] found that the nanocrystal luminescence decay time is not affected by the presence of Er. They argued that

* Corresponding author. Tel.: +31-20-6081234; fax: +31-20-6684106.

E-mail address: polman@amolf.nl (A. Polman).

0921-5107/01/$ - see front matter
PII: S0921-5107(00)00667-X

this would be inconsistent with the model in Fig. 1(a), since in this model erbium adds a non-radiative decay path for exciton recombination, which should lower the nanocrystal lifetime. (2) The *temperature dependence*: the nanocrystal luminescence intensity and the Er luminescence intensity are thought to be proportional to the excited concentration of excitons. Nevertheless, in temperature-dependent measurements [2,5] the Er luminescence intensity has repeatedly been observed to behave independently of the nanocrystal luminescence intensity. (3) The *excitation efficiency*: it is not known how efficiently exciton energy can be transferred to Er. (4) The *excitable Er fraction*: excitation via Si nanocrystals enhances the Er luminescence intensity, but it is not known which fraction of the Er is actually excitable. This knowledge is essential for the design of optical amplifiers and lasers based on Er- and nanocrystal-doped SiO_2. In this article these four points will be addressed and resolved.

2. Experimental

Silicon ions were implanted at 35 keV to a fluence of 6×10^{16} cm^{-2} into a 100-nm-thick SiO_2 layer that was formed by wet thermal oxidation of a lightly B-doped Si(100) substrate. The material was subsequently annealed at 1100°C for 10 min in vacuum at a base pressure below 3×10^{-7} mbar. This procedure is known to produce well-passivated Si nanocrystals in the size range 2–5 nm [6]. The corresponding nanocrystal concentration is approximately 10^{19} nanocrystals cm^{-3}. The nanocrystal-doped region was then implanted with different Er doses ranging from 3.6×10^{13} to 5.1×10^{15} cm^{-2} at a fixed energy of 125 keV. These implants result in an approximately Gaussian Er depth distribution, with Er peak concentrations ranging from 0.015 to 1.8 at.% at a depth of 61 nm. All samples were annealed at 1000°C in vacuum in order to remove implantation-induced damage. To further reduce defect-related luminescence, the material was passivated by performing an anneal at 800°C for 30 min in forming gas (H_2/N_2 at 1:9) at atmospheric pressure.

Photoluminescence (PL) spectra were measured using an Ar laser at 458 nm as excitation source. Excitation powers in the range 20 μW–10 mW were used in a ~1-mm diameter laser spot. The laser beam was modulated at 11 Hz using an acousto-optical modulator with a 100 ns cut-off time. The photoluminescence was focused onto the entrance slit of a grating monochromator and detected using standard lock-in techniques. Luminescence spectra were measured in the 600–1150 nm range using an AgOCs photomultiplier tube, and in the range 1100–1700 nm using a liquid-nitrogen cooled Ge detector. All spectra were corrected for the system response. Photoluminescence decay traces were recorded using either a photomultiplier in combination with a photon counting system, or a Ge detector in combination with a digitizing oscilloscope. The system response time in the two cases was 150 ns and 160 μs, respectively. The sample temperature was controlled between 15 and 300 K using a closed-cycle He cryostat.

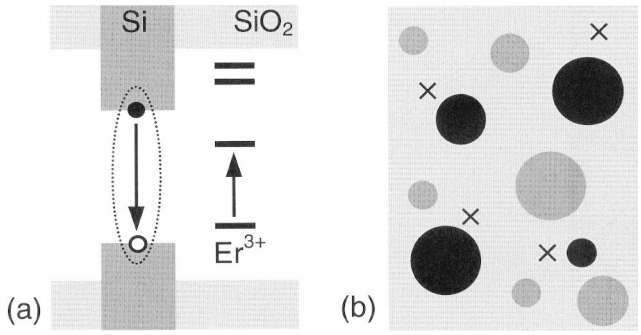

Fig. 1. (a) Schematic Er excitation model, showing the electronic band structure of Si nanocrystal-doped SiO_2 and the Er 4f energy levels. An optically generated exciton (dotted line) confined in the nanocrystal can recombine and excite Er^{3+}. (b) Schematic representation of SiO_2 containing Er (crosses) and nanocrystals (circles). The nanocrystals that couple to Er (filled circles) show no exciton luminescence.

3. Results and discussion

3.1. Nanocrystal–Er energy transfer rate and efficiency

Fig. 2 shows PL spectra taken at 20, 60, 180, and 300 K at a pump power of 10 mW for the sample with 1.8 at.% Er. At all temperatures a broad luminescence band is observed extending from 0.6 to 1.1 μm, which is attributed to radiative recombination of excitons localized at Si nanocrystals [6,7]. The exciton luminescence

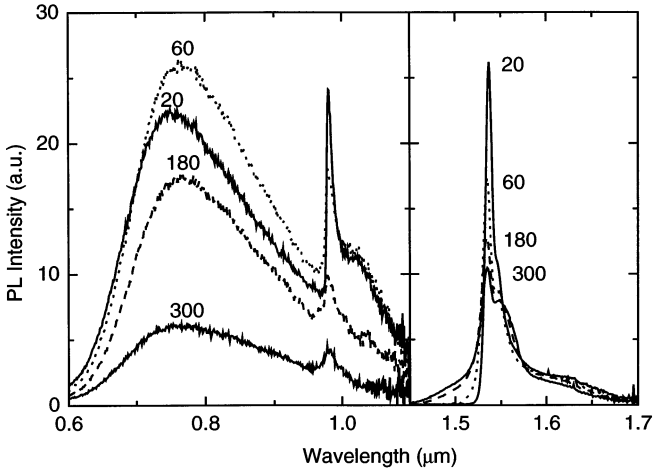

Fig. 2. Photoluminescence spectra at 20, 60, 180 and 300 K showing a broad nanocrystal spectrum in the range 600–1100 nm, and two clear Er luminescence lines at 982 and 1536 nm. The Er concentration was 1.8 at.%. $\lambda_{pump} = 458$ nm, 1 mW.

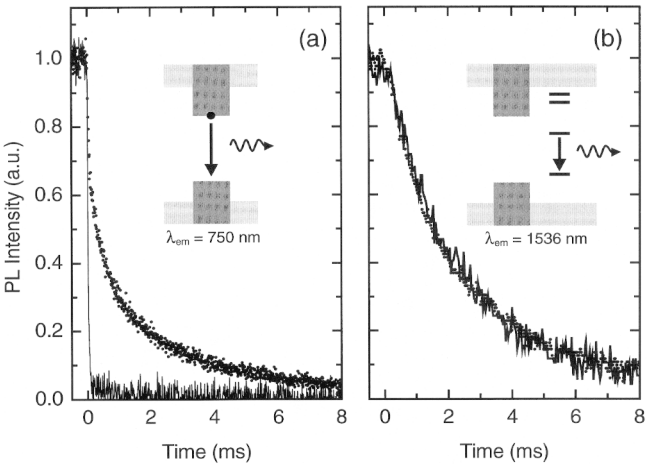

Fig. 3. Luminescence decay measurements taken at 15 K (dots) and at 300 K (drawn lines) of (a) nanocrystal luminescence at 750 nm, and (b) Er^{3+} luminescence at 1536 nm. $\lambda_{pump} = 458$ nm, 1 mW.

appears at energies above the bandgap energy of bulk Si due to quantum confinement [8]. The large spectral width of the nanocrystal luminescence is the result of the rather broad nanocrystal size distribution (diameter 2–5 nm).

Superimposed on the nanocrystal luminescence spectrum a relatively sharp peak is observed at 982 nm, corresponding to the $^4I_{11/2} \rightarrow {}^4I_{15/2}$ transition of Er^{3+}. Another clear emission line is observed at a wavelength of 1536 nm, corresponding to the $^4I_{13/2} \rightarrow {}^4I_{15/2}$ transition of Er^{3+}. Photoluminescence excitation spectra (not shown) indicate that the Er is not excited directly by optical absorption, but indirectly via an energy transfer process involving Si nanocrystals, as was shown before [1,2,5]. At a fixed pump power, the nanocrystal luminescence intensity and the Er luminescence intensity increase by a factor two when the excitation wavelength is decreased from 514 to 459 nm. We attribute this to the increasing nanocrystal optical absorption cross-section for increasing photon energy [9].

In Fig. 2 it can be seen that increasing the temperature from 20 to 300 K first causes the nanocrystal luminescence to increase by 16 % and then to decrease by 75% upon going from 60 to 300 K. This kind of temperature dependence is commonly observed for Si nanocrystals, and can be fully described [7] by a model that takes into account the temperature-dependent population of the exciton singlet and triplet states (with high and low radiative decay rate, respectively) in competition with non-radiative processes. The Er luminescence peak at 1536 nm exhibits an entirely different temperature dependence. The temperature increase only induces spectral broadening due to the thermal redistribution over the Stark levels, while the integrated intensity remains constant within 10%.

Fig. 3 shows luminescence decay curves of the nanocrystal luminescence at 750 nm and the Er luminescence at 1536 nm, measured at 15 and 300 K at a pump power of 1 mW for the same sample as in Fig. 2 (1.8 at.% Er). It is found that the nanocrystal decay rate (Fig. 3(a)) increases from 1.5×10^3 to 4.8×10^4 s^{-1} upon increasing the temperature from 15 to 300 K, which is consistent with the exciton singlet-triplet model [7]. The Er decay time at 1536 nm (Fig. 3(b)) is found to be 2.1 ms at all temperatures between 20 and 300 K, which implies that the Er luminescence efficiency is temperature-independent.

A consistent description of the observed temperature dependencies can be obtained if we assume *strong coupling* between a Si nanocrystal and Er. If the energy transfer from a nanocrystal to Er is fast, we expect to see no luminescence from a nanocrystal that is coupled to Er, since any generated exciton will immediately recombine non-radiatively by exciting Er. Such fast transfer might occur because at the high nanocrystal density ($\sim 10^{19}$ cm^{-3}) the maximum distance between an Er ion and the nearest nanocrystal is ~ 1 nm. The Er luminescence intensity will then be determined by the product of the nanocrystal absorption cross-section, which is approximately temperature-independent and the Er luminescence efficiency, which is also temperature-independent (Fig. 3(b)).

The fact that the Er luminescence intensity is constant up to room temperature implies that the energy transfer to Er occurs well within the nanocrystal decay time at 300 K, which is 21 μs. Consequently the transfer rate constant must be larger than $\sim 10^6$ s^{-1} at room temperature. This fast transfer explains the paradox encountered by Franzò et al. [5], who found that while the incorporation of Er does reduce the nanocrystal luminescence, it does not affect the nanocrystal decay time. This behavior is now expected, since in the strong-coupling case, all observed nanocrystal luminescence originates from nanocrystals that do not couple to Er, while nanocrystals that do couple to Er show no luminescence. This model is shown schematically in Fig. 1(b).

In order to determine the Er excitation efficiency, we measured the time-dependence of the nanocrystal and Er luminescence intensity as the pump beam is switched on and off, again for the sample with 1.8 at.% Er (Fig. 4). The curves measured upon switching on the pump show an initial rise followed by saturation, which corresponds to an initial increase in the population of excited Er followed by build-up of a steady state population. The curves upon switching off the pump probe the gradual decrease in excited Er population due to spontaneous decay. From the data in Fig. 4, taken at a pump power of 5 mW at 15 K, we derive the luminescence $1/e$ rise time (τ_r) and decay time (τ_d), from which we can deduce the excitation rate $R = (1/\tau_r - 1/\tau_d)$, assuming that the Er and the nanocrystals effectively behave as two level systems. At a pump intensity

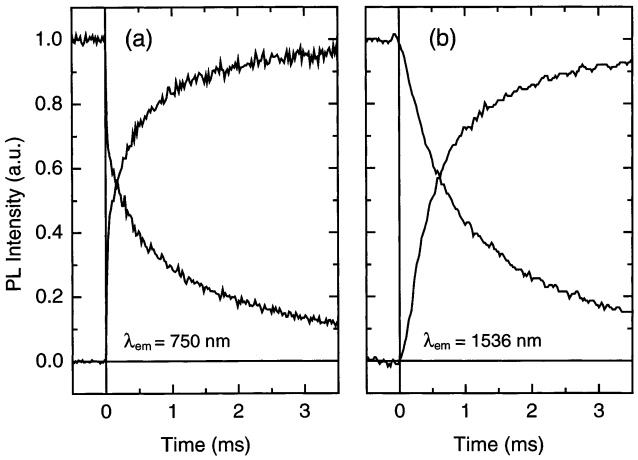

Fig. 4. PL intensity measured as the 5 mW pump beam is switched on and off, measured at 15 K for (a) nanocrystal luminescence at 750 nm, and (b) Er luminescence at 1536 nm. $\lambda_{pump} = 458$ nm.

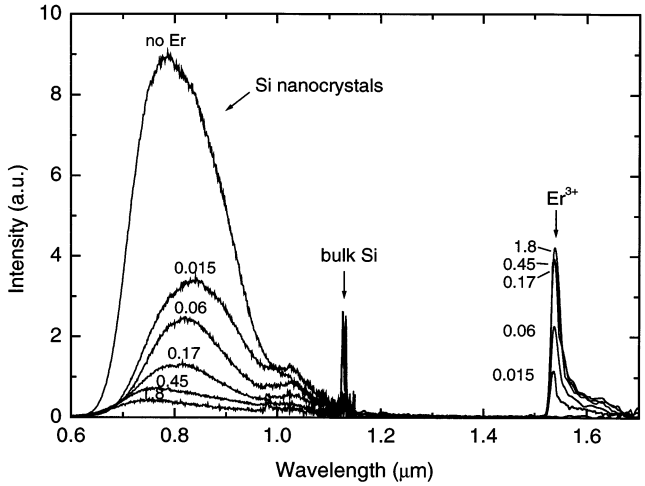

Fig. 5. Photoluminescence spectra of Si nanocrystal-doped SiO_2 containing different Er concentrations in the range 0–1.8 at.%, measured at 15 K using a pump power of 1 mW at 458 nm.

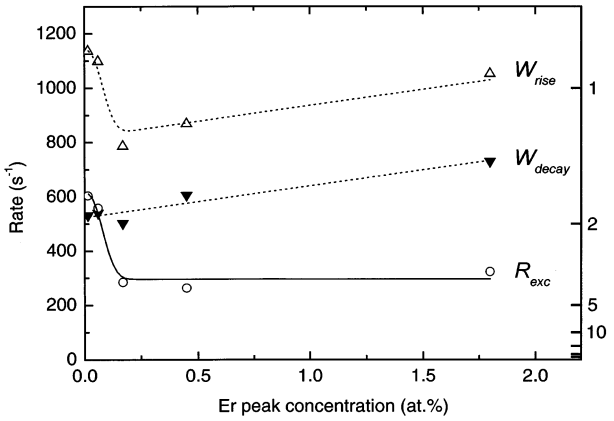

Fig. 6. Rise times (△) and decay times (▼) of the 1536 nm Er luminescence, measured at 15 K using a pump power of 1 mW at 458 nm, and the Er excitation rate derived from these data (○). The drawn lines serve as a guide to the eye.

of 5 mW mm^{-2} we find for the nanocrystal excitation rate $R_{nc} = 940\ s^{-1}$ and for the Er excitation rate $R_{Er} = 570\ s^{-1}$. Note that this Er excitation rate may contain a contribution of excitation into the higher lying Er energy levels, followed by non-radiative relaxation to the first excited state. Comparing the nanocrystal and Er excitation rates, we conclude that at least 60 % of the generated excitons recombine by transferring energy to Er [10]. This high conversion efficiency is in agreement with the strong coupling picture.

3.2. Er concentration limit

The high excitation efficiency also raises a new question. At the peak concentration of 1.8 at.% Er, the Er-to-nanocrystal ratio is approximately 100:1, which implies that in principle many Er ions compete for the same exciton. Nevertheless the observed Er excitation rate (*per ion)* is close to that of a single nanocrystal. This leads to the conclusion that a single nanocrystal can effectively excite only ~ 1–2 Er ions. This observation, together with the estimated nanocrystal concentration of $10^{19}\ cm^{-3}$, implies that the maximum excitable Er concentration is $\sim (1–2) \times 10^{19}\ cm^{-3}$ (~ 0.02–0.04 at.%).

In order to study this effect in more detail, PL spectra were taken of different samples with Er concentrations in the range 0.015–1.8 at.%. All data were taken at 15 K and are plotted in Fig. 5. A spectrum for a sample containing nanocrystals only is also shown in Fig. 5. It shows the broad luminescence due to the radiative recombination of quantum confined excitons in nanocrystals with a broad size distribution. The incorporation of 0.015 at.% Er reduces the nanocrystal luminescence by more than a factor two, and a luminescence peak due to Er appears at a wavelength of 1536 nm. Increasing the Er concentration leads to a further reduction of the nanocrystal luminescence intensity, accompanied by an increase of the Er luminescence intensity. This behavior is consistent with the strong coupling model, in which a nanocrystal becomes 'dark' once it couples to a nearby Er ion. Increasing the Er concentration therefore increases the fraction of dark nanocrystals. A saturation in the Er PL intensity is observed as the Er concentration exceeds 0.17 at.%. As can be seen in Fig. 5, even for the highest Er concentrations, some nanocrystal luminescence is observed. This is attributed to the fact that the Er implantation depth profile is slightly deeper than the Si depth profile [11], so that some nanocrystals in the near-surface region do not couple to Er.

In order to determine the concentration-dependent Er excitation rate, we performed rise time and decay time measurements of the Er luminescence at 1536 nm. At the applied pump power of 1 mW, all samples show approximately exponential time dependencies. Fig. 6

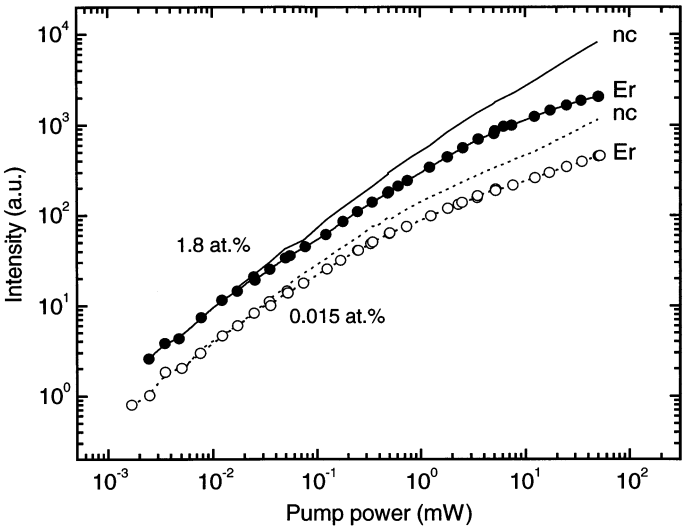

Fig. 7. Photoluminescence intensity of the nanocrystal luminescence at 750 nm and the Er luminescence at 1536 nm as a function of pump power for samples containing 0.015 and 1.8 at.% Er, measured at 15 K using 458 nm pump beam in a ~ 1 mm^2 spot.

shows the measured rates $W_r = 1/\tau_r$ and $W_d = 1/\tau_d$ obtained by exponential fitting of the data. The Er decay rate increases from 500 to 700 s^{-1} as the Er peak concentration is increased from 0.015 to 1.8 at.%. This increase is attributed to a concentration quenching effect that is known to occur when rare earth ions are spaced closely enough to allow for energy exchange between neighboring ions. As a result, excitation energy can migrate [12] to neighboring ions, which may in turn be coupled non-radiatively to quenching sites, e.g. defects or OH groups present in the matrix. In a simple concentration quenching model, the Er decay rate increases linearly with Er concentration, which is indeed observed in Fig. 6. By measuring the slope of the decay rate data in Fig. 6 we can estimate [13] that the concentration of quenching sites in the Er-implanted Si nanocrystal-doped SiO_2 film is as low as 10^{18} cm^{-3}.

Data for the Er excitation rate $R_{exc} = (1/\tau_r - 1/\tau_d)$ are also shown in Fig. 6. At an Er concentration of 0.015 at.%, the Er excitation rate is 600 s^{-1}. Increasing the Er concentration to 0.17 at.% reduces the excitation rate by a factor of two. A further increase of the Er concentration has no effect on the excitation rate, even though at these concentrations several Er ions might couple to the same nanocrystal, which would reduce the excitation rate per Er ion. The fact that such a reduction is not observed shows that there is an upper limit to the number of Er ions that can be excited by a single nanocrystal. From the data in Fig. 6 it is clear that this limit is reached at an Er concentration < 0.17 at.%. This is consistent with the limit of 0.02–0.04 at.% found above.

The data in Fig. 5 show a sub-linear increase of the Er intensity with concentration. This can be ascribed to the fact that as the Er concentration is increased, the exciton concentration available for Er excitation is reduced. At sufficiently high pump power however, the Er luminescence intensity is no longer limited by the exciton concentration but rather by the total amount of excitable Er. Therefore we can compare the total amount of excitable Er in samples with different Er concentrations by comparing Er luminescence intensities at high pump power.

Fig. 7 shows the pump power dependence of the Er (1536 nm) and nanocrystal (750 nm) luminescence intensity for samples containing 0.015 and 1.8 at.% Er, respectively. For both samples the nanocrystal luminescence intensity was scaled to coincide with the low-power Er luminescence intensity. Below 20 μW the Er luminescence and the nanocrystal luminescence depend linearly on pump power. At these low pump powers the Er luminescence intensities from the two samples differ by a factor of ~ 2. Increasing the pump power leads to a sublinear increase of the Er luminescence in both samples, suggesting that a significant fraction of the excitable Er is brought into the first excited state. At a pump power of 50 mW the nanocrystal luminescence continues to increase, while the Er luminescence intensity levels off. Hence, in this pump power regime the exciton generation rate is no longer the limiting factor for the Er luminescence intensity. Nevertheless, the Er luminescence intensities for the two samples at 50 mW pump power differ by only a factor of five, even though the total amount of Er in the samples differs by more than a factor of 100. This shows that the concentration of excitable Er in the high concentration (1.8 at.%) sample is at most five times higher than in the low concentration (0.015 at.%) sample, suggesting that the concentration of excitable Er is < 0.1 at.%. This is consistent with the concentration limit of < 0.17 at.% Er found above.

3.3. Models describing the Er concentration limit

The existence of an upper limit to the amount of excitable Er could indicate that there is a limit to the amount of *optically active* Er that can be incorporated in this material. This may for example be caused by Er clustering or $ErSi_2$ formation at the Si/SiO_2 interface, which would prevent the Er from being in the $3+$ valence state. However, measurements on Er and Si nanocrystal-doped waveguides show a strong Er^{3+} related absorption [14], suggesting that a large fraction of the Er is in the optically active state.

Alternatively, the observed concentration limit could be an intrinsic property of the excitation process. The amount of excitable Er will be low when the effective Er excitation efficiency is influenced by the presence of *excited* Er. Two models that would explain such a behavior are:

- *Auger de-excitation*, in which the already excited Er ion transfers its energy to an exciton generated in the nearby nanocrystal. A similar process has been shown to occur in Er-doped bulk Si [15]. After such Auger de-excitation the exciton can relax and subsequently excite an Er ion, effectively bringing the system back to the situation before the exciton was formed, or
- *pair-induced quenching*, in which two excited Er ions can interact yielding one Er ion in the $^4I_{9/2}$ state which rapidly decays to the first excited state, and one Er ion in the ground state. This co-operative upconversion effect usually causes a shortening of the Er decay rate at high pump powers, which has not been observed. However, if the Er–Er coupling is sufficiently strong, no effect on the lifetime is seen. This special case is usually called pair-induced quenching.

3.4. Device implications for a nanocrystal-sensitized Er-doped waveguide amplifier

From the measured Er excitation rate of $\sim 300\ s^{-1}$ at 1 mW (Fig. 6) we can determine an effective absorption cross-section σ_{eff} for the Er excitation process. We find that $\sigma_{eff} \approx 10^{-15}$ cm^2 at 458 nm, which is a factor 10^5–10^6 larger than what can be achieved using direct optical pumping of the Er ions, and similar to the Si nanocrystal absorption cross-section at a pump wavelength of 458 nm [9]. This high cross-section makes this nanocrystal sensitization concept ideal for application in waveguide amplifiers. Due to the wide nanocrystal absorption spectrum the pump wavelength can now be chosen over a broad spectral range. In fact, a broadband white light source may now be used as a pump source. The maximum gain of such a device is calculated to be 0.6 dB cm^{-1}, assuming a nanocrystal density of 10^{19} cm^{-3}, two Er ions per nanocrystal, and an Er emission cross-section [12] of 7×10^{-21} cm^2. We have recently fabricated Er and Si nanocrystal-doped waveguides in SiO_2 in which the index contrast is provided by the Si nanocrystals. The first measurements on these devices show excellent mode confinement and low optical losses.

4. Conclusions

We have shown evidence for strong coupling between excitons and Er in Si nanocrystal-doped SiO_2. The exciton–Er energy transfer is fast ($> 10^6\ s^{-1}$) and efficient (> 60 %). The maximum number of excitable Er ions around a single nanocrystal is 1–2, presumably due to an Auger de-excitation or a pair-induced quenching mechanism. This provides a fundamental limit to the amount of Er that can be excited in an Er-doped Si nanocrystal waveguide. At a typical nanocrystal concentration of 10^{19} cm^{-3}, the maximum optical gain at 1.54 μm of an Er-doped waveguide amplifier based on Si nanocrystal-doped SiO_2 is ~ 0.6 dB cm^{-1}. The effective Er excitation cross-section using this nanocrystal sensitization scheme is $\sigma_{eff} \approx 10^{-15}$ cm^2 at 458 nm, which is a factor 10^5–10^6 larger than the cross-section for direct optical pumping of Er. As the nanocrystal absorption spectrum extends over the full spectral range below ~ 1000 nm, this enables the fabrication of an Er-doped Si nanocrystal waveguide amplifier that can be pumped using a white light source.

Acknowledgements

This work is part of the research program of the Foundation for Fundamental Research on Matter (FOM) and was financially supported by the Netherlands Foundation for Scientific Research (NWO), the Dutch Technology Foundation (STW), and the SCOOP program of the European Union.

References

[1] M. Fujii, M. Yoshida, Y. Kanzawa, S. Hayashi, K. Yamamoto, Appl. Phys. Lett. 71 (1997) 1198.
[2] M. Fujii, M. Yoshida, S. Hayashi, K. Yamamoto, J. Appl. Phys. 84 (1998) 4525.
[3] J. St. John, J.L. Coffer, Y. Chen, R.F. Pinizzotto, J. Am. Chem. Soc. 121 (1888) 1998.
[4] C.E. Chryssou, A.J. Kenyon, T.S. Iwayama, C.W. Pitt, D.E. Hole, Appl. Phys. Lett. 75 (1999) 2011.
[5] G. Franzò, V. Vinciguerra, F. Priolo, Appl. Phys. A 69 (1999) 3.
[6] M.L. Brongersma, A. Polman, K.S. Min, E. Boer, T. Tambo, H.A. Atwater, Appl. Phys. Lett. 72 (1998) 2577.
[7] M.L. Brongersma, P.G. Kik, A. Polman, Appl. Phys. Lett. 76 (2000) 351.
[8] C. Delerue, G. Allan, M. Lannoo, Phys. Rev. B 48 (1993) 11024.
[9] D. Kovalev, J. Diener, H. Heckler, G. Polisski, N. Künzner, F. Koch, Phys. Rev. B 61 (2000) 4485.
[10] We assume that the nanocrystal absorption cross-section and spontaneous emission lifetime are not affected by the presence of Er.
[11] P.G. Kik, A. Polman, J. Appl. Phys. 88 (1992) 2000.
[12] W.J. Miniscalco, J. Lightwave Technol. 9 (1991) 234.
[13] F. Auzel, in: B. DiBartolo (Ed.), Radiationless Processes, Plenum, New York, 1980.
[14] P.G. Kik, A. Polman, Appl. Phys. Lett., submitted.
[15] F. Priolo, G. Franzò, S. Coffa, A. Carnera, Phys. Rev. B 57 (1998) 4443.